Intramolecular repulsion visible through the electrostatic potential in disulfides: Analysis via varying iso-density envelopes

Goedele Roos[1,*] & Jane S. Murray[2,*]

[1] Univ. Lille, CNRS, UMR 8576 - UGSF - Unité de Glycobiologie Structurale et Fonctionnelle, F-59000 Lille, France
[2]Department of Chemistry, University of New Orleans, New Orleans, LA 70148 USA

[*] **Corresponding authors**
Goedele Roos : Univ. Lille, CNRS, UMR, UGSF- Unité de Glycobiologie Structurale et Fonctionnelle, 8576, 50 avenue de Halley 59658 Villeneuve d'Ascq, F-59000 Lille, France, goedele.roos@univ-lille.fr
Jane S. Murray, Department of Chemistry, University of New Orleans, New Orleans, LA 70148 USA, jane.s.murray@gmail.com

Abstract

For a series of diethyl disulfide conformations, the nearly-touching contours of the electrostatic potential plotted on iso-density molecular surfaces allow the assessment of intramolecular repulsion. The electrostatic potential is plotted on varying iso-density envelopes to find the nearly-touching contours for which a) the surface electrostatic potential doesn't show overlap between atoms or functional groups and b) the typical features are visible (σ-hole, lone pair, hydrogen $V_{S,max}$). When these nearly-touching contours X are closer to the nuclei, the more electron density is excluded from the iso-density envelopes and the smaller are the volumes corresponding to these envelopes. Both the contours X and the corresponding volumes are found to correlate with relative conformational energy, reflecting the degree of intramolecular repulsion present in the various diethyl disulfides. Quantitative estimates of intramolecular repulsion can be made based on relationships between the nearly-touching contour X *vs*. relative energy and volume (of the nearly-touching contour X) *vs*. relative energy, obtained for series of diethyl disulfide conformers. These relations were used to analyze intramolecular repulsion in a set of disulfides broader than diethyl disulfide conformers. We have shown that the approach of varying electronic density contours can be used in the study of repulsive intramolecular interactions, hereby extending earlier work involving attractive intermolecular interactions.

Keywords

Disulfide, electrostatic potential, intramolecular interactions; iso-electronic density contours, conformational energy

Introduction

Interactions occurring within a molecule are called intramolecular [1]. The intramolecular forces hold the atoms together within a molecule, resulting in what are often called ionic, covalent or metallic bonds. Weaker interactions such as hydrogen-bonding and van der Waals interactions can also be present intramolecularly. For example, large molecules such as proteins and DNA strands are structured by these types of interactions, and they are found also within small molecules. Examples are *ortho*-nitroaniline, **1** and *ortho*-chlorophenol, **2**. One of the amine hydrogens in **1** interacts attractively with the closest nitro-oxygen, while in **2,** the hydroxyl hydrogen interacts attractively with the negative side of the nearby chlorine atom. In both cases, the intramolecular interactions affect chemical and physical properties of the molecules [2], such as acidities and hydrogen bond-donating tendencies.

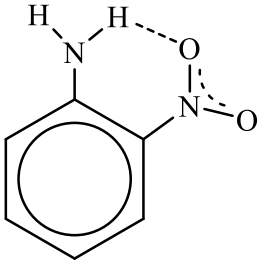

1

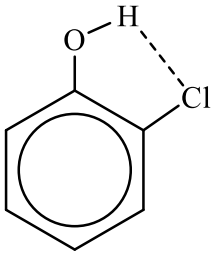

2

Intramolecular interactions are in contrast to intermolecular interactions; in the latter a portion or portions of one molecule interacts with a region or regions of space of another molecule. For example, DNA-protein, protein-protein complexes and protein-ligand interactions are structured by both intra- and intermolecular non-covalent interactions [3] as are materials that are directionally-bound via halogen bonding and other σ- and π-hole interactions [4–7] .

In this contribution we are focusing upon intramolecular interactions, which are difficult to quantify because unlike intermolecular interactions, there is only one molecular species involved[1] which cannot be straightforwardly separated into interacting fragments. Therefore, energy decomposition analyses (EDA) and symmetry-adapted perturbation theory (SAPT) approaches have been used extensively to study intermolecular interactions [8–11], but have only occasionally extended to intramolecular interactions[12]. In this paper we will be presenting an approach that does not require separating a molecule into parts. For further reading on EDA and SAPT, we also refer to the references given in the cited papers.

Following the Hellmann-Feynman theorem [13–15], the intramolecular forces that hold the atoms together within a molecule or molecular complex, whether they be ionic, covalent or metallic bonds or the weaker interactions mentioned above, are Coulombic in nature [16–21]. The force exerted upon any nucleus is the classical electrostatic force due to the other nuclei and the electron density distribution; thus, the attractive interactions of each nucleus are with the electrons and the repulsive ones are with the other nuclei, while electron-electron interactions are by nature repulsive. This follows from the Schrödinger equation, where all terms in the

Hamiltonian are Coulombic and from the fact that the wave function is an eigenfunction of the Hamilton operator. For a comprehensive derivation of the Hellmann-Feynman theorem, see Politzer *et al*.[15].

Intramolecular interactions as H-bonds are attractive in nature [22]; however, repulsive intramolecular interactions may also be present within molecules. An illustrative example thereof is the strained 'staple' conformation (**3**) a disulfide - formed by the interaction between the sulfur atoms of two cysteine amino acids - can adopt in proteins. Examples are the redox enzyme disulfide binding protein D-alpha (DsbD α) of *E. coli*; the disulfide formed in neurotoxin type B of *C. botulinum* or in agglutenin of *Anguilla Anguilla* (see further Table 2). In these disulfide-staples, a repulsive interaction is present between the end -CH_3 groups coming as close as ~ 3.9 Å to each other. In these conformations, the six heavy atoms form a 6-membered ring, adopting a conformation resembling a 'staple' (**3**).

The conformation of the catalytic disulfide formed, for example in the reductase protein thioredoxin (Trx), is a very stable low energy disulfide conformation (**4**). Here, no repulsive interactions are present and Trx preferentially crystallizes in its disulfide (oxidized) form. The disulfide conformation in which the heavy atoms form a 5-membered ring, the eclipsed conformation (**5**), was previously identified [23] as a TS for rotation around the disulfide bond.

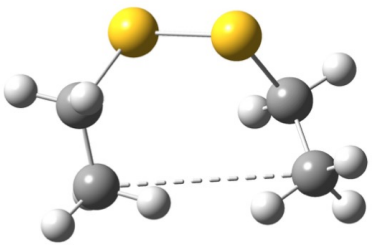

3

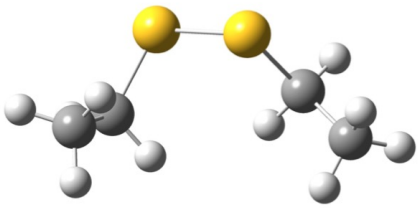

4

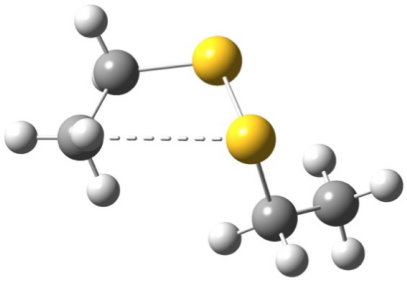

5

Protein disulfides can thus adopt a wide variety of conformations, each having different relative energies [24–27] to which the disulfide redox potentials are directly linked [23]. Strained disulfide

conformations in which intramolecular repulsion is present, such as staple-disulfides (see **3**), have high conformational energies and a strong tendency to be reduced. Here, the unfavorable repulsive interactions are released upon reduction of the disulfide to di-thiol [23].

Starting with diethyl disulfides in different conformations as model systems, in this contribution, we investigate whether the electrostatic potential plotted on iso-density surfaces can be used as a tool to make intramolecular repulsion visible. Varying contours of the electronic density have been used in earlier work to asses *attractive inter*molecular interactions [28,29]. Here, we extend this to assess *repulsive intra*molecular interactions.

Electrostatic potential and varying contours

The electrostatic potential V(**r**) that is produced at any point **r** by the nuclei and electrons of a molecule is expressed rigorously by eq. (1):

$$V(\mathbf{r}) = \sum_A \frac{Z_A}{|\mathbf{R}_A - \mathbf{r}|} - \int \frac{\rho(\mathbf{r}')d\mathbf{r}'}{|\mathbf{r}' - \mathbf{r}|} \qquad (1)$$

Z_A is the charge on nucleus A, located at $\mathbf{R_A}$ and $\rho(\mathbf{r})$ is the molecule's electronic density. Eq. (1) shows that V(**r**) is the sum of a positive contribution due to the nuclei and a negative one from the electrons; its sign in any particular region depends, therefore, upon whether the effects of the nuclei or electrons are dominant in that region [30].

The electrostatic potential V(**r**) is a real physical property, an observable. It can be determined experimentally, by diffraction techniques [31–33], as well as computationally. It is important to recognize that the value of the potential at any point **r** reflects contributions from all of the nuclei and electrons of the molecule [34–36]. Among the consequences of this are that the electrostatic potential does not always follow the electron density, i.e. electron-rich regions do not necessarily have negative potentials, and the positive potentials due to σ-holes may not be directly at the positions of the most diminished electronic density (σ-hole) [37].

The electrostatic potential V(**r**) is often computed on an iso-density surface, following Bader *et al.* [38], defined by the 0.001 a. u. or similar contour of its electronic density [34] and is labeled $V_S(\mathbf{r})$. The locally most positive and most negative values, of which there may be several on a given molecular surface, are designated as $V_{S,max}$ and $V_{S,min}$ respectively.

A key observation regarding the electrostatic potentials of most organic molecules containing hydrogens is that each hydrogen will have an accessible hemispherical positive region of electrostatic potential with a surface maximum, or $V_{S,max}$ [22,34,39], unless the hydrogen is involved in an intramolecular interaction [1,40]. In cases where the hydrogen is involved in an intramolecular interaction, there is either no visible $V_{S,max}$ on the surface or one that has a smaller than expected magnitude; see Figure 1(a). The four phenyl hydrogens of *ortho*-

chlorophenol (**2**) each have hemispherical surfaces around them, while the hydroxyl hydrogen does not (Figure 1(a)). This is a clue that this hydrogen is involved in an intramolecular interaction, in this case with the side of the negative chlorine. The hydrogen $V_{S,max}$ observed on most hydrogens in organic molecules (and others) are typically along the extension of the bond to the hydrogen and result from the diminished electronic density (σ-hole) in that region of space [7,22].

Look now at Figure 1(b). Figure 1(b) shows the potential of **2** on a contour of the electronic density much closer to the nuclei, the 0.018 a. u. contour, where the hydroxyl hydrogen is shown to be hemispherical, and the chlorine also has its typical shape. In this paper we refer to such contours as the nearly-touching contours.

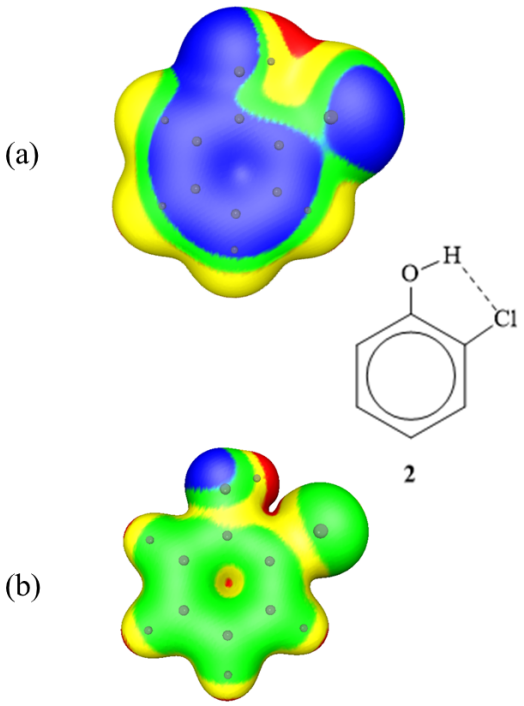

Figure 1. Computed electrostatic potentials on the (a) 0.001 a. u. and (b) 0.018 a. u. molecular surfaces, respectively, of *ortho*-chlorophenol (**2**). Gray spheres denote the positions of the atoms, corresponding to structure **2**. Color ranges: red, greater than 15; yellow, between 15 and 0; green, between 0 and -5; blue, more negative than -5. The hydroxyl group is at the top with the chloro substituent to the top right. View (b) resolves the driving forces for the H---Cl intramolecular interaction in **2**; these cannot be clearly identified in view (a).

Computational methods and model systems

In the present study, electrostatic potentials were computed at the density functional B3PW91/6-31(d,p) level, using Gaussian 09 [41,42] and the WFA-SAS [43] code. This procedure has been shown to be reliable for computing electrostatic potentials [44]. Prior to the electrostatic potential calculations, all geometries are optimized and energies are calculated at the MP2/6-31++G(d,p) level with Gaussian 09 [41,42].

Three series of model systems were selected and built:

Series 1 consists of diethyl disulfide adopting different conformations; DEDS (Table 1). The conformation of diethyl disulfide $CH_3CH_2S–SCH_2CH_3$ can be characterized by the dihedral angels: χ2, χ3 and χ2' (see Scheme 1). Note that the structure of CH_3CH_2S-SCH_2CH_3 is symmetrical with equivalent χ2 and χ2'. Therefore, the conformations (χ2, χ3, χ2') and (χ2', χ3, χ2) have the same energy.

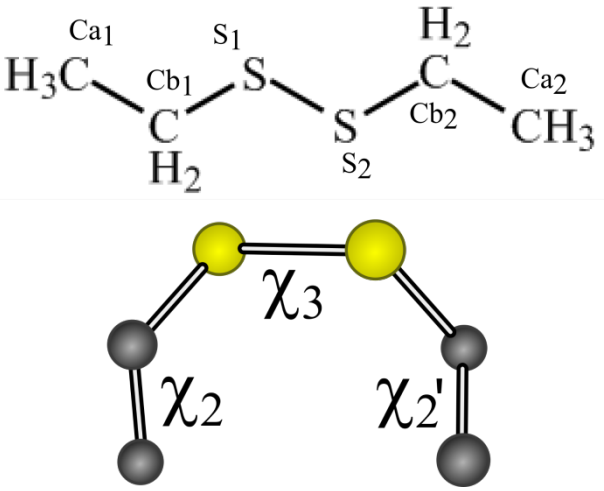

Scheme 1: Numbering of the C and S atoms and of the χ2, χ3 and χ2' angles in diethyl-disulfide.

The diethyl disulfides with different conformations were fully optimized (R) or fully optimized with fixed dihedral angles (F).

For series 2, the conformations of diethyl disulfides were taken directly from PDB structures; PDB (Table 2). For these structures, only the H-atoms were placed and subsequently optimized.

For both of these series, relative energies are obtained in relation to the lowest energy conformation, DEDS2, adopting dihedral angles (68,87,68).

For Series 3, in addition to diethyl disulfide in its lowest energy conformation, a variety of commercially available disulfides were selected and fully optimized; S3 (Scheme 2).

Table 1 : Series 1, the diethyl-disulfides, DEDS. Relative energies ΔE_{rel} (kcal/mol) are calculated (MP2/6-311++G(d,p)) with respect to the fully optimized lowest energy structure reference structure DEDS2, adopting dihedral angles (68,87,68).
The intramolecular interaction distances d are given in Ångstroms; F: optimized with fixed dihedral angles; R: optimized with relaxed dihedral angles

Name	Dihedral angles of starting structures $\chi_2, \chi_3, \chi_{2'}$	Dihedral angles after optimization $\chi_2, \chi_3, \chi_{2'}$	ΔE_{rel} kcal/mol	d(S_1- S_2) Å	d(Ca_1-Ca_2) Å	d(S_1-Ca_2) d(S_2-Ca_1) Å
DEDS1	60,90,60	F	0.46	2.058	5.59	3.41 3.41
DEDS2**	60,90,60	R: 68,87,68	0.00	2.060	5.70	3.49 3.49
DEDS3	-60,90,-60	F*	5.73	2.061	**3.30**	3.68 3.68
DEDS4	-25,90,-60	F*	6.98	2.056	**3.31**	3.61 3.43
DEDS5	-60,90,-60	R: -71,111,-71	2.05	2.068	3.58	3.59 3.59
DEDS6	60,90,-5	F*	4.09	2.053	**4.90**	**2.96** 3.43

* Structures having one imaginary frequency, after optimization at the MP2/6-311++G(d,p) level

** Reference structure

Table 2: Series 2: PDB: Examples from the Protein Data Base. Relative energies ΔE_{rel} (kcal/mol) are calculated (MP2/6-311++G(d,p)) with respect to the reference structure DEDS2, *cfr*. Table 1. The intramolecular interaction distances d are given in Ångstroms.

Name	Protein	PDB	Dihedral angles after optimization $\chi_2, \chi_3, \chi_{2'}$	* ΔE_{rel} kcal/mol	d(S_1- S_2) Å	d(Ca_1-Ca_2) Å	d(S_1-Ca_2) d(S_2-Ca_1) Å
PDB1	*S. aureus* Trx (WT)	2o7k Cys32-Cys35	81,74,-146	3.6	2.036	5.32	3.70 4.34
PDB2	*E. coli* DsbD-alpha	1jpe Cys103-Cys109	-77,93,-112	3.5	2.038	**3.88**	3.68 4.11
PDB3	*E. coli* Grx1	2c1r Cys27-Cys30	-142,80,71	4.1	2.064	5.21	3.69 4.37
PDB4	*E. coli* Trx	1xoa Cys32-Cys35	74,76,-146	3.1	2.070	5.24	3.72 4.32
PDB5	*C. botulinum* neurotoxin type B	1epw Cys436-Cys445	-106,98,-81	4.1	2.031	**3.98**	3.77 4.05
PDB6	*Anguilla Anguilla* agglutinin	1k12 Cys82-Cys83	91,-88,83	6.0	2.053	**3.74**	3.97 3.85

* Calculated after placing and optimization of the H-atoms at the MP2/6-311++G(d,p) level.

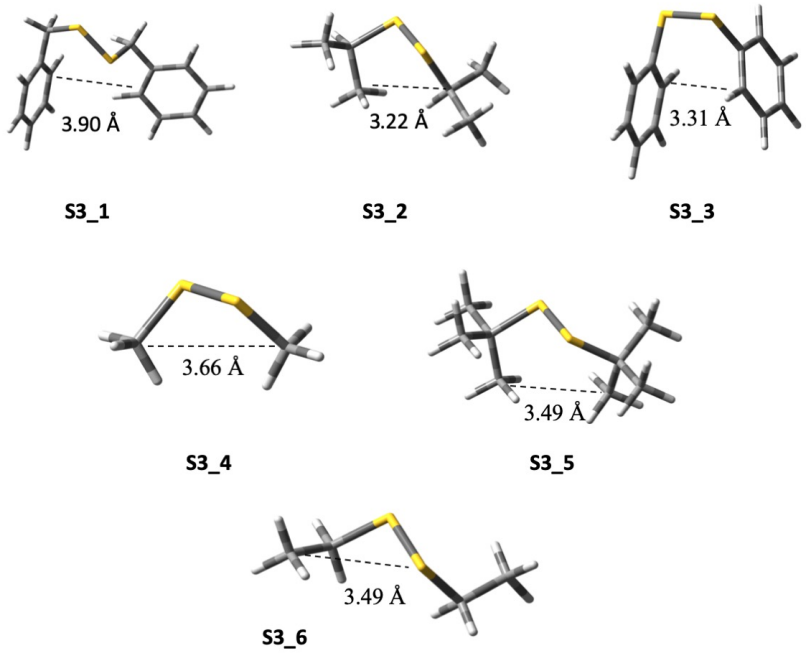

Scheme 2: Series 3: Dibenzyl disulfide (**S3_1**); Di-isopropyl disulfide (**S3_2**); Di-phenyl disulfide (**S3_3**); Dimethyl disulfide (**S3_4**); Di-*tert*-butyl disulfide (**S3_5**); Diethyl disulfide (**S3_6**).

Results and discussion

Exploring varying iso-density envelopes

Following Bader *et al*. [38], for all of the conformers/molecules of the three series mentioned in the Methods section, we first have looked at the electrostatic potential on the envelope or surface around the molecule at the standard contour of the electron density (0.001 a. u.). We anticipated that each molecule at the 0.001 a. u. contour might have a $V_{s,max}$ for each hydrogen, as is normal for non-interacting hydrogens in organic molecules [22,34]. This is indeed found in some of the conformations studied (DEDS1, Figure 2 I. a). In other cases, the information is hidden within the 0.001 a. u. contour envelope (Figure 2 I. b-d) and so, accordingly, a $V_{S,max}$ is not visible on each of the ten H-atoms. Here, we need to plot the electrostatic potential on contours closer to the nuclei to 'free' the hydrogen atoms. For example, for the eclipsed conformation DEDS6 and for PDB1, the nearly-touching contours are respectively the 0.0053 a. u. and the 0.0075 a. u. contour (Figure 2 II. c and d).

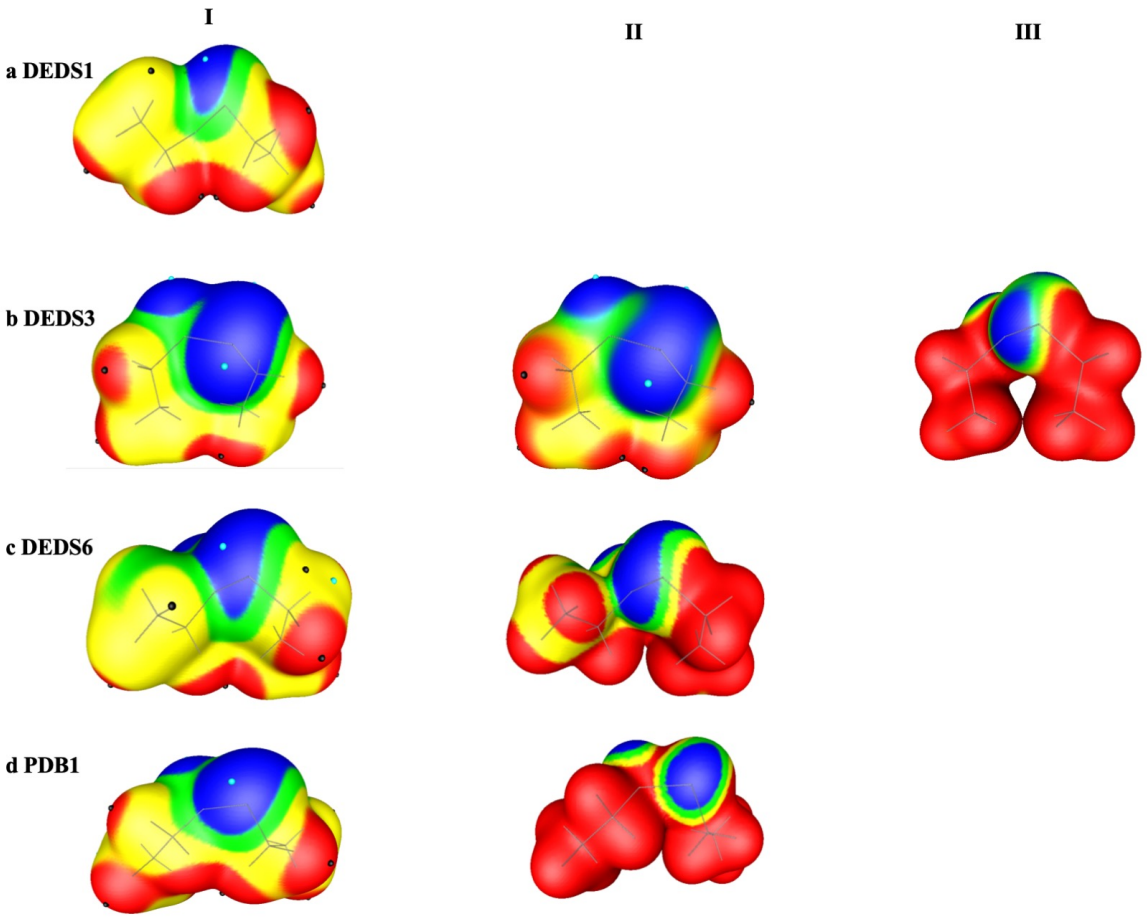

Figure 2*:* **I** Examples of the electrostatic potential plotted at the 0.001 a. u. contour for which $V_{S,max}$ is **a** visible and **b-d** not visible on all H-atoms (**a** DEDS1; **b** DEDS3; **c** DEDS6; **d** PDB1). **a** Each sulfur atom has a $V_{S,min}$, designated by light blue hemispheres and each hydrogen atom

has a $V_{S,max}$, designated by black hemispheres; **b-d** Each sulfur atom has a $V_{S,min}$, designated by light blue hemispheres and only 9 of the 10 H-atoms have a $V_{S,max}$, designated by black hemispheres.
II b DEDS3: electrostatic potential plotted on the 0.002 a. u. contour, all 10 H-atoms have a $V_{S,max}$, but methyl groups are not separated; **c** DEDS6: electrostatic potential plotted on the 0.0053 a. u. contour, all 10 H-atoms have a $V_{S,max}$ and methyl groups are separated; **d** PDB1: electrostatic potential plotted on the 0.0075 a. u., all 10 H-atoms have a $V_{S,max}$. **III b** DEDS3: electrostatic potential plotted on the 0.0093 a. u. contour, all 10 H-atoms have a $V_{S,max}$ and methyl groups are separated. The color ranges for all surface electrostatic potentials, in kcal/mol, are: red, greater 10; yellow, from 10 to 0; green, from 0 to -10; blue, more negative than -10.

For the staple conformation, the contours for which the $V_{S,max}$ of each H atom is visible, are not enough to free all overlapping electron density (Figure 2 II. b). For the DEDS3 conformation, for example, the $V_{S,max}$ on all H-atoms is already visible at the 0.002 a. u. contour (Figure 2 II. b). However, for this contour, the electrostatic potential of the methyl groups still overlaps. In order to 'separate' the methyl groups, we need to go deeper into the envelope and look for contours on which the electrostatic potential of the methyl groups is nearly touching. For the DEDS3 example, this is the 0.0093 a. u. contour (Figure 2 III. b). This essentially says that more electron density must be excluded from the surface envelopes in order to first make the $V_{S,max}$ visible on each H-atom and next to separate the electrostatic potential of the methyl groups from each other. Otherwise stated, the electron densities overlap at surfaces with a lower iso-electron density value, thus laying farther away from the nuclei, indicating intramolecular repulsion. Furthermore, one can see that the nearly touching groups have both a positive potential (indicated by the red color in Figure 2), repelling each other; for the attractive interactions in Figure 1, the electrostatic potential of the nearly touching groups is positive on the -OH side and negative on the -Cl side.

Previous work assigned the high relative energies (~6-7 kcal/mol) of the staple conformations as DEDS3 and DEDS4, having a small d(Ca_1-Ca_2) of ~3.3 Å (Table 1), to steric hindrance between the terminal $–CH_3$ groups [23]. The repulsive interactions were described in terms of an energy decomposition analysis in which the so-called Pauli repulsion [45,46] dominates. Here, we rigorously showed by means of the electrostatic potential on iso-density surfaces that indeed, electron densities are overlapping, which is repulsive by nature. This shows that the classical electrostatic force is indeed able to capture "all" information, including repulsive intramolecular interactions. Coulomb's law is thus sufficient to explain covalent and non-covalent interactions. This was already pointed out in intermolecular contexts [19,28,29], for example the attractive interaction in complexes between aromatic molecules and HCN [36]. In this work, we have extended this finding to intramolecular repulsive interactions.

Note that for DEDS1 and DEDS2, even though the $V_{s,max}$ on all H-atoms are already visible on the 0.001 a. u. contour, a better separation of the electrostatic potential of the closest hydrogens

can be obtained at the 0.002 a. u. and/or 0.003 a. u. contours. For these contours, the shapes of the regions around the closest hydrogens are more hemispherical (Figure 3).

Historically, for the purpose of plotting properties such as the electrostatic potential on a molecular surface to mimic what an approaching molecule would 'see', the 0.001 a. u. iso-density surface was chosen for following reasons: **1**) The 0.001 a. u. surface is generally farther from the atoms than the often-used van der Waals radii (except for hydrogen); and **2**) There was a slightly better correlation between hydrogen $V_{S,max}$ values and the Kamlet-Taft hydrogen-bond donating parameters at the 0.001 a. u. contour [47].

Since Bader *et al*. showed that the space within the 0.003 a. u. iso-density surface envelope was found to well represent the molecular volume of organic molecules [38], we can take here the 0.003 a. u. isodensity surface as our reference value to identify repulsive interactions in diethyl disulfides: if the nearly-touching contour is found at a value higher than 0.003 a. u., thus closer to the nuclei, the volumes, and thus the electron densities overlap.

Table 3 gives a complete overview of the nearly-touching contours by which repulsive interactions are identified; Figure 2 shows representative examples.

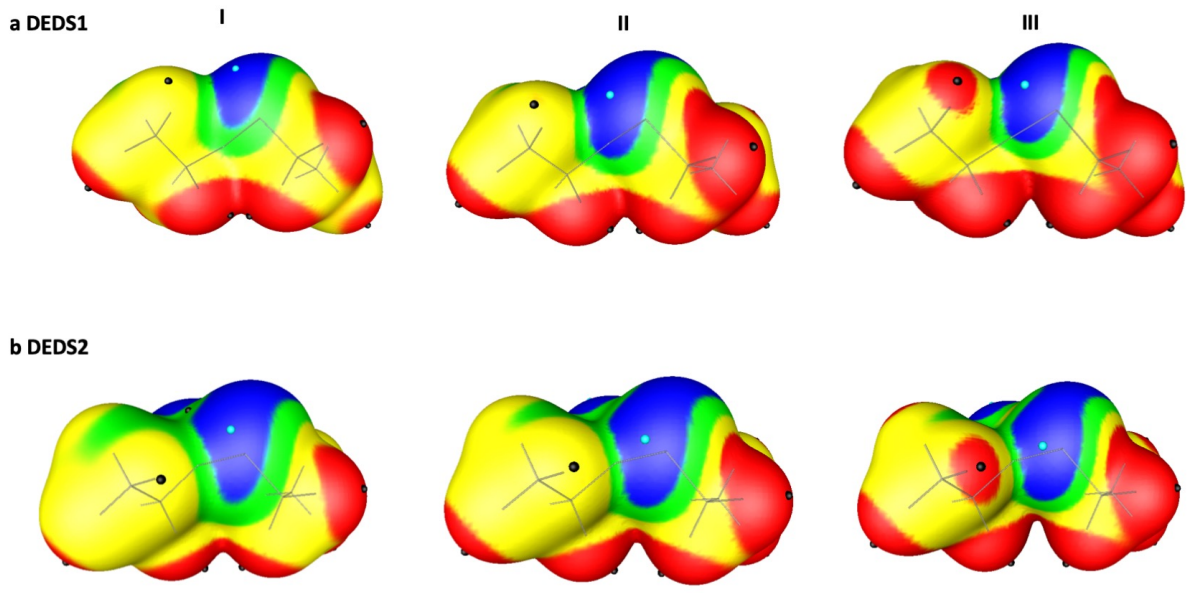

Figure 3: Separation of the electrostatic potential of the closest hydrogens plotted at the 0.001 a. u. (**I**) 0.002 a. u. (**II**) and 0.003 a. u. (**III**) iso-density surface for DEDS1 (**a**) and DEDS2 (**b**). The color ranges, in kcal/mol, are: red, greater 10; yellow, from 10 to 0; green, from 0 to -10; blue, more negative than -10.

Table 3: Overview of the nearly-touching contours of the diethyl disulfide conformers from Series 1 and 2: the contour at which the $V_{S,max}$ is visible for all H-atoms or the contours at which the electrostatic potential of the methyl groups is separated. The conformations in *italics* are identified as conformations in which *intramolecular* repulsion is present, based on the 0.003 a. u. isodensity surface criterium for separation of the electron-density.

Series 1	Dihedral angles after optimization $\chi_2, \chi_3, \chi_{2'}$	Contour (a.u.)	ΔE_{rel} (kcal/mol)	Volume at contour X (Å^3)
DEDS1	60,90,60	0.003	0.46	120.46
DEDS2	68,87,68	0.003	0.00	120.26
DEDS3	-60,90,-60	0.0093	5.73	79.87
DEDS4	-25,90,-60	0.0105	6.98	76.02
DEDS5	-71,*111*,-71	0.0063	2.05	93.18
DEDS6	60,90,-5	0.0053	4.09	99.36
Series 2	Dihedral angles after optimization $\chi_2, \chi_3, \chi_{2'}$	Contour (a.u.)	ΔE_{rel} (kcal/mol)	Volume at contour X (Å^3)
PDB1	81,74,-146	0.0075	3.56	86.83
PDB2	-77,93,-112	0.01	3.46	77.44
PDB3	-142,80,71	0.0075	4.06	86.84
PDB4	74,76,-146	0.006	3.06	94.55
PDB5	-106,98,-81	0.0082	4.06	83.84
PDB6	91,-88,83	0.0148	5.96	65.73

Quantifying intra-molecular interactions

To assess the intramolecular interactions, weather they are favorable or disfavor able we can look at the electrostatic potential plots on varying contours, as pointed out in the previous section. Furthermore, quantitative relationships exist between volumes at the nearly-touching contour X and relative conformational energy (Figure 4) and between the values of the nearly-touching contour X and relative conformational energy (Figure 5). Thus, as the nearly-touching contour X increases (is closer to the nuclei) and the corresponding volume decreases, the more intramolecular repulsion is present in the diethyl disulfides, resulting in higher conformational energies.

MP2 conformational energies may be criticized for including also attractive contributions as London dispersion, instead of quantifying the repulsion in the exact sense, as would for example HF energies do. As mentioned in the introductory section, the sign of the electrostatic potential in any particular region depends, upon whether the effects of the nuclei or electrons are dominant in that region [30]. In the same way, the conformational energy can be viewed as a consequence of both the attractive interactions (as dispersion interactions between methyl groups coming closer together) and of the repulsive interactions, present in this particular conformation. As such, the overall resulting conformational energy is either attractive or repulsive, depending on weather the attractive or repulsive terms dominate. A high relative conformational energy (thus a large positive value), indicates that the repulsive term dominates compared to the lowest energy conformation (taken as reference, having the value: 0.0 kcal/mol), even after the subtraction of the attractive terms. This dominance of the repulsive terms is what is referred to as intra-molecular repulsion throughout the manuscript.

Figure 4 and 5 generalizes what was found before for attractive intermolecular interactions [28]. For the attractive bimolecular A---B complexes, the nearly-touching contours of the electronic densities have been proposed as encompassing the impenetrable volumes of A and B in the complexes. It was found that the smaller the impenetrable volumes are, the stronger are the interactions in the complexes [28]. When you go to contours closer to the nuclei and compute the volumes, you are removing electronic density and thus volume from everywhere. However, the volume decrease and also the excluded electronic charge of the electronic density does correlate with the interaction energy [28,29]. This is attributed to more volume decrease and thus more excluded electronic charge in the region of the interaction.

The present work thus shows that our approach can be extended to repulsive intramolecular interactions.

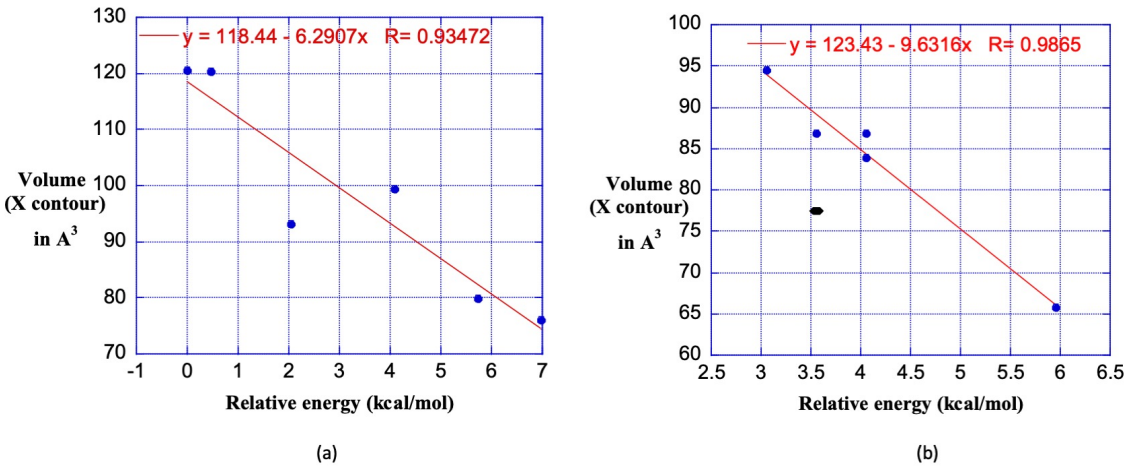

Figure 4. Plots of the nearly-touching contour X *vs*. relative energy of a conformer: **a** the DEDS series; **b** the PDB series (the data point for outlier PDB2 is shown, but was not included in the linear regression).

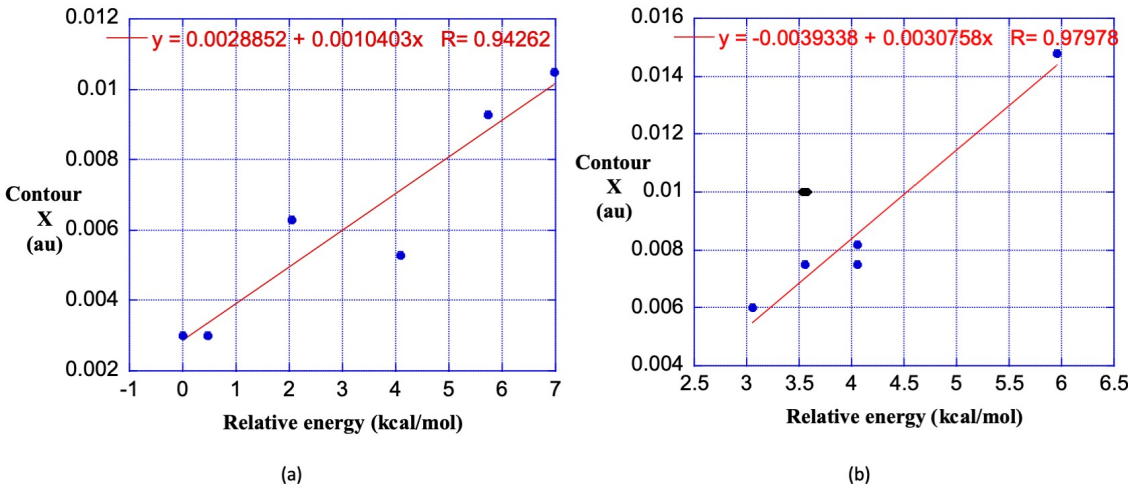

Figure 5. Plots of the nearly-touching contour X *vs*. relative energy of a conformer: **a** the DEDS series; **b** the PDB series (the data point for outlier PDB2 is shown, but was not included in the linear regression).

Estimation of intramolecular repulsion in a new set of disulfides

Can we now use the insight and the relationship established in Figure 5(a) to analyze a new set of molecules? In Series 3 we have considered, in addition to diethyl disulfide in its fully optimized, lowest energy conformation, five other commercially available disulfides (Scheme 2). For each molecule, one conformation is picked as a simple test. A full study on the whole conformational space should be performed to make an absolute classification of intramolecular repulsion present in these molecules. Overall, the separation we obtain between disulfide, diethyl disulfide and di-isopropyl disulfide showing no intramolecular repulsion and di-*tert*-butyl disulfide, diphenyl disulfide and dibenzyl disulfide showing significant intramolecular repulsion will hold and indicates that we can reasonably say something when applying our proposed approach.

For dimethyl disulfide, diethyl disulfide and di-isopropyl disulfide conformation, all 10 H-atoms have hydrogen $V_{S,max}$ visible on the 0.001 a. u. contour, however to be consistent with the DEDS Series in Table 3, we are basing our estimates of the intramolecular repulsion for these on the 0.003 a. u. cut-off established in the DEDS series; no significant intramolecular repulsion is present in the conformation studied for these molecules.

For the picked di-*tert*-butyl disulfide, diphenyl disulfide and dibenzyl disulfide conformations, the electrostatic potential plotted at the 0.001 a. u. contour shows significant overlap of electronic density (Figure 6), pointing to the presence of intramolecular repulsion in these molecules.

For di-*tert*-butyl disulfide, an interaction between two hydrogens, one on each *tert*-butyl group can be noted; the nearly-touching contour resolving this interaction can be found at 0.0062 a. u. For diphenyl disulfide, all H-atoms have a $V_{S,max}$ on the 0.001 a. u. contour, but the phenyl rings overlap. The nearly-touching contour for this molecule is at the 0.01 a. u. iso-density surface. For dibenzyl disulfide, at the 0.001 a. u. contour, there is an interaction between a C-H on the benzyl group with the ring of the other benzyl group. Here, the nearly-touching contour can be found at 0.0056 a. u.

The quantitative estimates of the intramolecular repulsion from the nearly-touching contours using the linear regression of Figure 5(a) for the conformation studied of dibenzyl disulfide, diphenyl disulfide and di-tert-butyl disulfide are respectively 2.6, 6.8 and 3.2 kcal/mol. These values are much higher than the relative energy estimate of 0.1 kcal/mol for dimethyl disulfide, diethyl disulfide and di-isopropyl disulfide, molecules for which the nearly-touching contours reveal the absence of intramolecular repulsion (see above). For these quantitative estimates, it is necessary to use Figure 5(a), which involves the contours X *vs*. relative energy relationship. The volume *vs*. relative energy relationships (Figure 4) in this study can only be used to make predictions for conformers, such as the DEDS series, because volume is an extensive property.

Table 4: Nearly-touching contours at which the hydrogen $V_{S,max}$ are visible for all H-atoms and for which there is no overlap of the electrostatic potential between groups. Estimates of the intramolecular repulsion (kcal/mol) of the molecules from the linear regressions obtained for the DEDS series plots (Figure 5**a**).

Name	Contour (a. u.)	Estimates of intramolecular repulsion (from Figure 5**a**) (kcal/mol)
Dibenzyl disulfide (**S3_1**)	0.0056	2.6
Di-isopropyl disulfide (**S3_2**)	0.003	0.1
Diphenyl disulfide (**S3_3**)	0.01	6.8
Dimethyl disulfide (**S3_4**)	0.003	0.1
Di-*tert*-butyl disulfide (**S3_5**)	0.0062	3.2
Diethyl disulfide (**S3_6**)	0.003	0.1

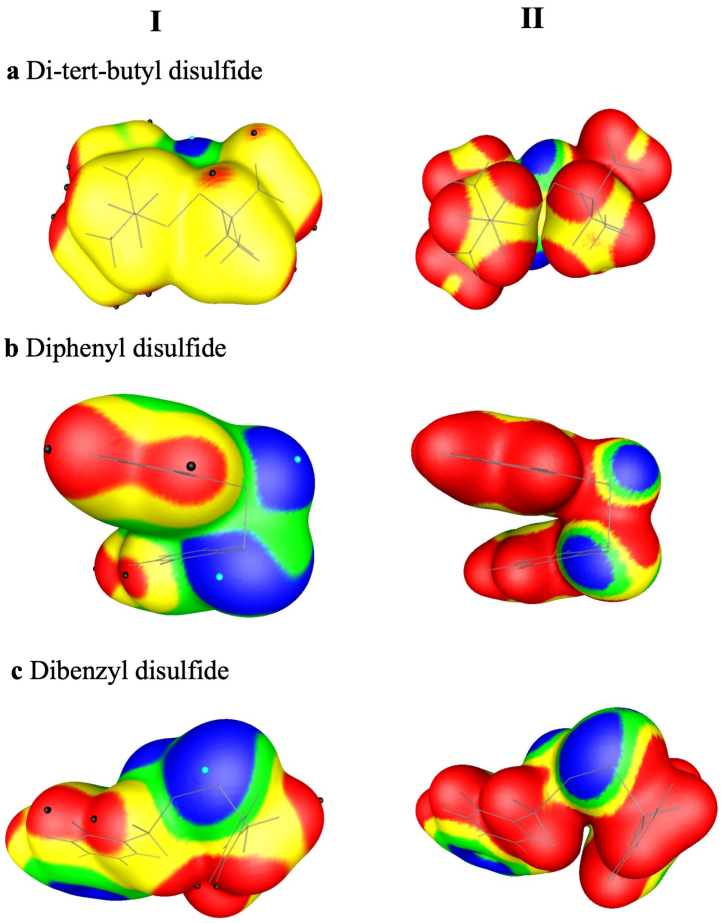

Figure 6: **I** Electrostatic potential plotted on the 0.001 a. u. contour for **a** Di-tert-butyl disulfide, **b** Diphenyl disulfide and **c** Dibenzyl disulfide. **II** Nearly-touching contours for the electrostatic potential at **a** 0.0062 a. u., **b** 0.01 a. u., **c** 0.0056 a. u. iso-density surfaces. The color ranges, in kcal/mol, are: red, greater 10; yellow, from 10 to 0; green, from 0 to -10; blue, more negative than -10.

The electrostatic potential gives the correct picture regarding the presence of intramolecular repulsion

As shown in the previous sections, intramolecular repulsion, giving high conformational energies, can unambiguously be detected by the electrostatic potential plotted on varying contours of the electronic density. On the other hand, high conformational energies are not always due to the presence of intramolecular repulsion. We will discuss two examples of diethyl disulfide conformations for which the high conformational energy can mistakenly be appointed to the presence of intramolecular repulsion. For these examples, the electrostatic potential and not the conformational energy gives the correct picture regarding the absence of intramolecular repulsion.

Conformations in which χ2 (or χ2') adopts a value of ~120° or -120° have high relative energies. The DEDS-TS1 and DEDS-TS2 conformations (Table 5 I. a) are examples thereof. In proteins, these conformations are stabilized by the protein scaffold and are present in the PDB structures, as for example PDB-TS3 and PDB-TS4 (Table 5 I. b). Analyzing the electrostatic potentials for these molecules shows that already at the 0.001 a. u. contour, the electrostatic potential has a $V_{S,max}$ for all H-atoms, pointing to the absence of intramolecular repulsion. When going to the 0.002 a. u. and the 0.003 a. u. contours, a better separation of the surface electrostatic potentials is obtained (Figure 7a).
In these diethyl disulfides conformations, similar intramolecular interaction distances (Table 5 I. a-b) as in the reference structure with the lowest energy conformation are found and earlier work pointed out that these conformations are transition states for rotation around the S–S bond [23]. As such, the electrostatic potential is able to correctly detect here the absence of repulsive intramolecular interactions.

Also diethyl disulfide conformations with χ3 angles outside the favorable zone, which was identified before to be between 70° and 120° [23,48,49], have a high relative energy. For example, DEDS-C1 (Table 5 II. a) and PDB-C2 (Table 5 II. b), having a χ3 angle of -142°. Here as well, the electrostatic potential shows correctly that no intramolecular repulsion is present for these conformations as the nearly-touching contour can already be found at the 0.001 a. u. iso-density surface (Figure 7b). Instead, in these conformations a substantially smaller S-S bond length is present, giving rise to high conformational energies.

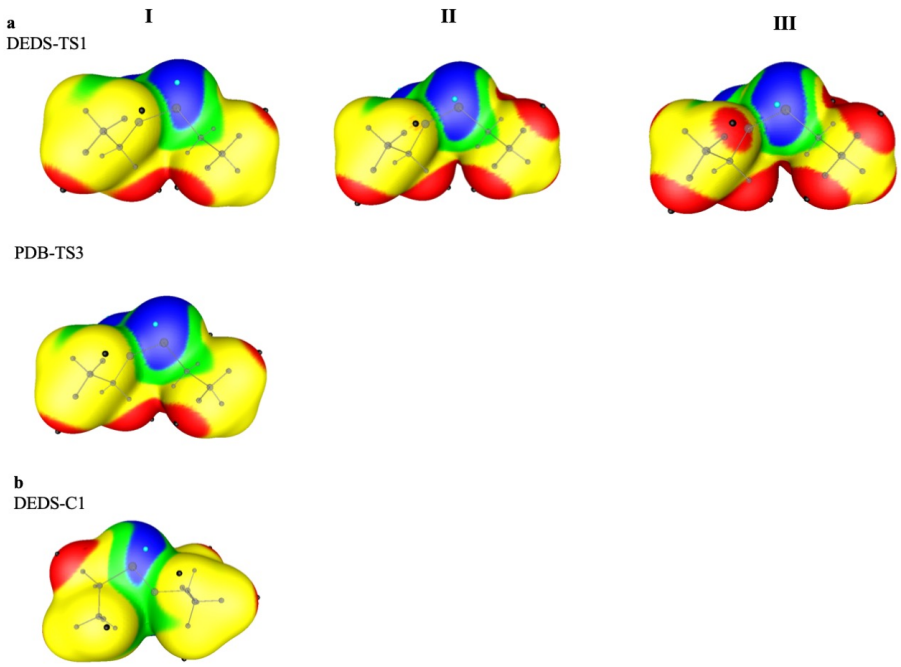

Figure 7: Representative examples (*cfr.* Table 5) of **a** diethyl disulfides with conformations in which χ2 (or χ2') adopts a value of ~120° or -120° and of **b** diethyl disulfides with conformations in which χ3 adopts a value outside the favourable 70° < χ3 < 120° region. Electrostatic potential plotted on the 0.001 a. u. (**I**), the 0.002 (**II**) a. u. and the 0.003 (**III**) a. u.

contour. The color ranges, in kcal/mol, are: red, greater 10; yellow, from 10 to 0; green, from 0 to -10; blue, more negative than -10.

Table 5: I. Examples of diethyl disulfides with conformations in which χ2 (or χ2') adopts a value of ~120° or -120° **II**. Examples of diethyl disulfides with conformations in which χ3 adopts a value outside the favourable 70° < χ3 < 120° region.
a The DEDS series and **b** the PDB series.
All relative energies (kcal/mol) are calculated (MP2/6-311++G(d,p)) with respect to reference structure DEDS2, *cfr*. Table 1.
The intramolecular interaction distances d are given in Ångstroms.

a

Name	Dihedral angles after optimization $\chi_2, \chi_3, \chi_{2'}$	E_{rel} kcal/mol	d (S_1- S_2) Å	d (Ca_1-Ca_2) Å	d (S_1-Ca_2) d (S_2-Ca_1) Å	Contour a. u.
I						
DEDS-TS1*	67,86,-125	2.27	2.058	4.90	3.48 4.48	0.001
DEDS-TS2*	-67,-86,125	2.27	2.058	4.90	3.48 4.18	0.001
II						
DEDS-C1*	60,-140,60	5.40	**2.090**	4.31	3.38	0.001

*Optimized to a TS at the MP2/6-311++G(d,p) level, with relaxed dihedral angles.

b

Name	Protein	PDB	E_{rel}* kcal/mol	Dihedral angles after optimization $\chi_2, \chi_3, \chi_{2'}$	d(S_1- S_2) Å	d(Ca_1-Ca_2) Å	d(S_1-Ca_2) d(S_2-Ca_1) Å	Contour a. u.
I								
PDB-TS3	Human Hemochromatosis protein	1de4 (C-chain) Cys556-Cys558	3.8	70,92,-**127**	2.049	5.42	3.77 4.02	0.001
PDB-TS4	*N. meningitides* DsbA1 – T176V mutant	3hz8 Cys57-Cys60	4.8	77,75,-**134**	2.091	5.16	3.67 4.32	0.001
II								
PDB-C2	Human Cdc25B	1cwr Cys426-Cys473	20.1	43,-**142**,78	**1.957**	5.09	3.57 4.80	0.001

* Calculated after placing and optimization of the H-atoms at the MP2/6-311++G(d,p) level.

Conclusion

For the disulfide systems under study, we have shown that searching for the nearly-touching contour of the electronic density as the contour upon which to plot the electrostatic potential provides a useful tool for assessing intramolecular repulsion. The electrostatic potentials of the neighboring groups at these contours show clearly that the interactions are repulsive in nature. For the diethyl disulfides, quantitative estimates of conformational energy can be made using linear relations with both the contour values and the volumes of the envelope.

The present work extends what was found before for *attractive* intermolecular interactions to intramolecular *repulsion*. It shows here that the approach of searching for the non-overlapping electrostatic potentials on varying iso-electron density envelopes has the potential to be generally used to assess both attractive and repulsive inter- and intramolecular interactions.

Table of Contents Image

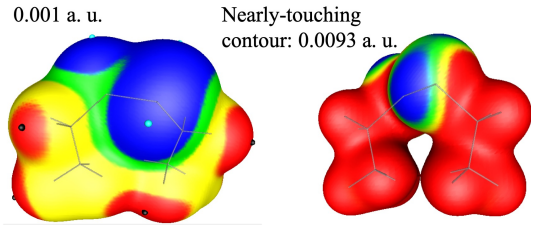

Corresponding Authors

Goedele Roos : Univ. Lille, CNRS, UMR, UGSF- Unité de Glycobiologie Structurale et Fonctionnelle, 8576, 50 avenue de Halley 59658 Villeneuve d'Ascq, F-59000 Lille, France, goedele.roos@univ-lille.fr

Jane S. Murray : Department of Chemistry, University of New Orleans, New Orleans, LA 70148 USA, jane.s.murray@gmail.com

Author Contributions

The manuscript was written through contributions of all authors. All authors have given approval to the final version of the manuscript.

Acknowledgements

The computational resources and services used in this work were partially provided by the Centre de Ressources Informatiques (CRI), Univ. Lille.

J. S. M. would like to acknowledge the many years of inspiration and encouragement given to her by the late Peter Politzer, particularly in the area of noncovalent interactions and varying contours of the electronic density.

References

(1) Politzer, P.; Murray, J. S. Non-Hydrogen-Bonding Intramolecular Interactions: Important but Often Overlooked. In *Practical Aspects of Computational Chemistry I*; Leszczynski, J., Shukla, M. K. K., Eds.; Springer Netherlands: Dordrecht, 2011; pp 479–496. https://doi.org/10.1007/978-94-007-0919-5_16.

(2) Panunto, T. W.; Urbanczyk-Lipkowska, Z.; Johnson, R.; Etter, M. C. Hydrogen-Bond Formation in Nitroanilines: The First Step in Designing Acentric Materials. *J. Am. Chem. Soc.* **1987**, *109* (25), 7786–7797. https://doi.org/10.1021/ja00259a030.

(3) Jena, S.; Dutta, J.; Tulsiyan, K. D.; Sahu, A. K.; Choudhury, S. S.; Biswal, H. S. Noncovalent Interactions in Proteins and Nucleic Acids: Beyond Hydrogen Bonding and π-Stacking. *Chem. Soc. Rev.* **2022**, *51* (11), 4261–4286. https://doi.org/10.1039/D2CS00133K.

(4) Auffinger, P.; Hays, F. A.; Westhof, E.; Ho, P. S. Halogen Bonds in Biological Molecules. *Proc. Natl. Acad. Sci. U.S.A.* **2004**, *101* (48), 16789–16794. https://doi.org/10.1073/pnas.0407607101.

(5) Murray, J. S.; Lane, P.; Clark, T.; Riley, K. E.; Politzer, P. σ-Holes, π-Holes and Electrostatically-Driven Interactions. *J Mol Model* **2012**, *18* (2), 541–548. https://doi.org/10.1007/s00894-011-1089-1.

(6) Bauzá, A.; Mooibroek, T. J.; Frontera, A. The Bright Future of Unconventional σ/π-Hole Interactions. *ChemPhysChem* **2015**, *16* (12), 2496–2517. https://doi.org/10.1002/cphc.201500314.

(7) Politzer, P.; Murray, J. S.; Clark, T.; Resnati, G. The σ-Hole Revisited. *Phys. Chem. Chem. Phys.* **2017**, *19* (48), 32166–32178. https://doi.org/10.1039/C7CP06793C.

(8) Morokuma, K. Why Do Molecules Interact? The Origin of Electron Donor-Acceptor Complexes, Hydrogen Bonding and Proton Affinity. *Acc. Chem. Res.* **1977**, *10* (8), 294–300. https://doi.org/10.1021/ar50116a004.

(9) Reed, A. E.; Curtiss, L. A.; Weinhold, F. Intermolecular Interactions from a Natural Bond Orbital, Donor-Acceptor Viewpoint. *Chem. Rev.* **1988**, *88* (6), 899–926. https://doi.org/10.1021/cr00088a005.

(10) Misquitta, A. J.; Podeszwa, R.; Jeziorski, B.; Szalewicz, K. Intermolecular Potentials Based on Symmetry-Adapted Perturbation Theory with Dispersion Energies from Time-Dependent Density-Functional Calculations. *The Journal of Chemical Physics* **2005**, *123* (21), 214103. https://doi.org/10.1063/1.2135288.

(11) Mao, Y.; Loipersberger, M.; Horn, P. R.; Das, A.; Demerdash, O.; Levine, D. S.; Prasad Veccham, S.; Head-Gordon, T.; Head-Gordon, M. From Intermolecular Interaction Energies and Observable Shifts to Component Contributions and Back Again: A Tale of Variational Energy Decomposition Analysis. *Annu. Rev. Phys. Chem.* **2021**, *72* (1), 641–666. https://doi.org/10.1146/annurev-physchem-090419-115149.

(12) Sproviero, E. M. Intramolecular Natural Energy Decomposition Analysis: Applications to the Rational Design of Foldamers. *J. Comput. Chem.* **2018**, *39* (20), 1367–1386. https://doi.org/10.1002/jcc.25127.

(13) *Hans Hellmann: Einführung in die Quantenchemie: Mit biografischen Notizen von Hans Hellmann jr.*; Andrae, D., Ed.; Springer: Berlin, Heidelberg, 2015. https://doi.org/10.1007/978-3-662-45967-6.

(14) Feynman, R. P. Forces in Molecules. *Phys. Rev.* **1939**, *56* (4), 340–343. https://doi.org/10.1103/PhysRev.56.340.

(15) Politzer, P.; Murray, J. S. The Hellmann-Feynman Theorem: A Perspective. *J Mol Model* **2018**, *24* (9), 266. https://doi.org/10.1007/s00894-018-3784-7.

(16) Slater, J. C. Hellmann-Feynman and Virial Theorems in the *X* α Method. *The Journal of Chemical Physics* **1972**, *57* (6), 2389–2396. https://doi.org/10.1063/1.1678599.
(17) Bader, R. F. W. *Atoms in Molecules: A Quantum Theory*; Oxford University Press: Oxford, 1990.
(18) Rahm, M.; Hoffmann, R. Distinguishing Bonds. *J. Am. Chem. Soc.* **2016**, *138* (11), 3731–3744. https://doi.org/10.1021/jacs.5b12434.
(19) Clark, T.; Murray, J. S.; Politzer, P. A Perspective on Quantum Mechanics and Chemical Concepts in Describing Noncovalent Interactions. *Phys. Chem. Chem. Phys.* **2018**, *20* (48), 30076–30082. https://doi.org/10.1039/C8CP06786D.
(20) Politzer, P.; Murray, J. S. A Look at Bonds and Bonding. *Struct Chem* **2019**, *30* (4), 1153–1157. https://doi.org/10.1007/s11224-019-01364-3.
(21) Brown, D. Another Look at Bonds and Bonding. *Struct Chem* **2020**, *31* (1), 1–5. https://doi.org/10.1007/s11224-019-01433-7.
(22) Murray, J. S.; Politzer, P. Hydrogen Bonding: A Coulombic σ-Hole Interaction. *J Indian Inst Sci* **2020**, *100* (1), 21–30. https://doi.org/10.1007/s41745-019-00139-3.
(23) Roos, G.; Fonseca Guerra, C.; Bickelhaupt, F. M. How the Disulfide Conformation Determines the Disulfide/Thiol Redox Potential. *J. Biomol. Struct. & Dyn.* **2015**, *1*, 93–103.
(24) Wouters, M. A.; George, R. A.; Haworth, N. L. "Forbidden" Disulfides: Their Role as Redox Switches. *Curr Protein Pept Sci* **2007**, *8* (5), 484–495.
(25) Haworth, N. L.; Feng, L. L.; Wouters, M. A. High Torsional Energy Disulfides: Relationship between Cross-Strand Disulfides and Right-Handed Staples. *J Bioinform Comput Biol* **2006**, *4* (1), 155–168.
(26) Wouters, M. A.; Fan, S. W.; Haworth, N. L. Disulfides as Redox Switches: From Molecular Mechanisms to Functional Significance. *Antioxid Redox Signal* **2010**, *12* (1), 53–91. https://doi.org/10.1089/ARS.2009.2510.
(27) Haworth, N. L.; Gready, J. E.; George, R. A.; Wouters, M. A. Evaluating the Stability of Disulfide Bridges in Proteins: A Torsional Potential Energy Surface for Diethyl Disulfide. *Molecular Simulations* **2007**, *33* (6), 475–485.
(28) Murray, J. S.; Politzer, P. In Search of the 'Impenetrable' Volume of a Molecule in a Noncovalent Complex. *Molecular Physics* **2018**, *116* (5–6), 570–577. https://doi.org/10.1080/00268976.2017.1353711.
(29) Murray, J. S.; Zadeh, D. H.; Lane, P.; Politzer, P. The Role of 'Excluded' Electronic Charge in Noncovalent Interactions. *Molecular Physics* **2019**, *117* (17), 2260–2266. https://doi.org/10.1080/00268976.2018.1527044.
(30) Politzer, P.; Daiker, K. C. ChemInform Abstract: Models for Chemical Reactivity (318 Literaturangaben). *Chemischer Informationsdienst* **1982**, *13* (13). https://doi.org/10.1002/chin.198213377.
(31) Stewart, R. F. On the Mapping of Electrostatic Properties from Bragg Diffraction Data. *Chemical Physics Letters* **1979**, *65* (2), 335–342. https://doi.org/10.1016/0009-2614(79)87077-3.
(32) *Chemical Applications of Atomic and Molecular Electrostatic Potentials: Reactivity, Structure, Scattering, and Energetics of Organic, Inorganic, and Biological Systems*; Politzer, P., Truhlar, D. G., Eds.; Springer US: Boston, MA, 1981. https://doi.org/10.1007/978-1-4757-9634-6.
(33) Stevens, E. D.; Klein, C. L. Charge Density Studies of Drug Molecules. In *The Application of Charge Density Research to Chemistry and Drug Design*; Jeffrey, G. A., Piniella, J. F., Eds.; NATO ASI Series; Springer US: Boston, MA, 1991; Vol. 250, pp 319–336. https://doi.org/10.1007/978-1-4615-3700-7_13.

(34) Murray, J. S.; Politzer, P. Molecular Electrostatic Potentials and Noncovalent Interactions. *WIREs Comput Mol Sci* **2017**, *7* (6). https://doi.org/10.1002/wcms.1326.
(35) Wheeler, S. E.; Houk, K. N. Through-Space Effects of Substituents Dominate Molecular Electrostatic Potentials of Substituted Arenes. *J. Chem. Theory Comput.* **2009**, *5* (9), 2301–2312. https://doi.org/10.1021/ct900344g.
(36) Murray, J. S.; Shields, Z. P.-I.; Seybold, P. G.; Politzer, P. Intuitive and Counterintuitive Noncovalent Interactions of Aromatic π Regions with the Hydrogen and the Nitrogen of HCN. *Journal of Computational Science* **2015**, *10*, 209–216. https://doi.org/10.1016/j.jocs.2015.02.001.
(37) Politzer, P.; Murray, J. S. σ-Holes and π-Holes: Similarities and Differences. *J. Comput. Chem.* **2018**, *39* (9), 464–471. https://doi.org/10.1002/jcc.24891.
(38) Bader, R. F. W.; Carroll, M. T.; Cheeseman, J. R.; Chang, C. Properties of Atoms in Molecules: Atomic Volumes. *J. Am. Chem. Soc.* **1987**, *109* (26), 7968–7979. https://doi.org/10.1021/ja00260a006.
(39) Murray, J. S.; Politzer, P. Correlations between the Solvent Hydrogen-Bond-Donating Parameter .Alpha. and the Calculated Molecular Surface Electrostatic Potential. *J. Org. Chem.* **1991**, *56* (23), 6715–6717. https://doi.org/10.1021/jo00023a045.
(40) Göbel, M.; Tchitchanov, B. H.; Murray, J. S.; Politzer, P.; Klapötke, T. M. Chlorotrinitromethane and Its Exceptionally Short Carbon–Chlorine Bond. *Nature Chem* **2009**, *1* (3), 229–235. https://doi.org/10.1038/nchem.179.
(41) M. J. Frisch, G. W. T., H. B. Schlegel, G. E. Scuseria, M. A. Robb, J. R. Cheeseman, G. Scalmani, V. Barone, B. Mennucci, G. A. Petersson, H. Nakatsuji, M. Caricato, X. Li, H. P. Hratchian, A. F. Izmaylov, J. Bloino, G. Zheng, J. L. Sonnenberg, M. Hada, M. Ehara, K. Toyota, R. Fukuda, J. Hasegawa, M. Ishida, T. Nakajima, Y. Honda, O. Kitao, H. Nakai, T. Vreven, J. A. Montgomery, Jr. ,. J. E. Peralta, F. Ogliaro, M. Bearpark, J. J. Heyd, E. Brothers, K. N. Kudin, V. N. Staroverov, R. Kobayashi, J. Normand, K. Raghavachari, A. Rendell, J. C. Burant, S. S. Iyengar, J. Tomasi, M. Cossi, N. Rega, J. M. Millam, M. Klene, J. E. Knox, J. B. Cross, V. Bakken, C. Adamo, J. Jaramillo, R. Gomperts, R. E. Stratmann, O. Yazyev, A. J. Austin, R. Cammi, C. Pomelli, J. W. Ochterski, R. L. Martin, K. Morokuma, V. G. Zakrzewski, G. A. Voth, P. Salvador, J. J. Dannenberg, S. Dapprich, A. D. Daniels, Ö. Farkas, J. B. Foresman, J. V. Ortiz, J. Cioslowski, and D. J. Fox. Gaussian 09, Revision A.1; Gaussian, Inc.: Wallingford CT, 2009.
(42) Frisch, M. J. ; T., G. W. ;. Schlegel, H. B. ;. Scuseria, G. E. ;. Robb, M. A. ;. Cheeseman, J. R. ;. Scalmani, G. ;. Barone, V. ;. Mennucci, B. ;. Petersson, G. A. ;. Nakatsuji, H. ;. Caricato, M. ;. Li, X. ;. Hratchian, H. P. ;. Izmaylov, A. F. ;. Bloino, J. ;. Zheng, G. ;. Sonnenberg, J. L. ;. Hada, M. ;. Ehara, M. ;. Toyota, K. ;. Fukuda, R. ;. Hasegawa, J. ;. Ishida, M. ;. Nakajima, T. ;. Honda, Y. ;. Kitao, O. ;. Nakai, H. ;. Vreven, T. ;. Montgomery, J. A. ,. Jr. ;. Peralta, J. E. ;. Ogliaro, F. ;. Bearpark, M. ;. Heyd, J. J. ;. Brothers, E. ;. Kudin, K. N. ;. Staroverov, V. N. ;. Kobayashi, R. ;. Normand, J. ;. Raghavachari, K. ;. Rendell, A. ;. Burant, J. C. ;. Iyengar, S. S. ;. Tomasi, J. ;. Cossi, M. ;. Rega, N. ;. Millam, N. J. ;. Klene, M. ;. Knox, J. E. ;. Cross, J. B. ;. Bakken, V. ;. Adamo, C. ;. Jaramillo, J. ;. Gomperts, R. ;. Stratmann, R. E. ;. Yazyev, O. ;. Austin, A. J. ;. Cammi, R. ;. Pomelli, C. ;. Ochterski, J. W. ;. Martin, R. L. ;. Morokuma, K. ;. Zakrzewski, V. G. ;. Voth, G. A. ;. Salvador, P. ;. Dannenberg, J. J. ;. Dapprich, S. ;. Daniels, A. D. ;. Farkas, Ö. ;. Foresman, J. B. ;. Ortiz, J. V. ;. Cioslowski, J. ;. Fox, D. J. Gaussian 09, 2009.
(43) Bulat, F. A.; Toro-Labbé, A.; Brinck, T.; Murray, J. S.; Politzer, P. Quantitative Analysis of Molecular Surfaces: Areas, Volumes, Electrostatic Potentials and Average Local

Ionization Energies. *J Mol Model* **2010**, *16* (11), 1679–1691. https://doi.org/10.1007/s00894-010-0692-x.

(44) Riley, K. E.; Tran, K.-A.; Lane, P.; Murray, J. S.; Politzer, P. Comparative Analysis of Electrostatic Potential Maxima and Minima on Molecular Surfaces, as Determined by Three Methods and a Variety of Basis Sets. *Journal of Computational Science* **2016**, *17*, 273–284. https://doi.org/10.1016/j.jocs.2016.03.010.

(45) Bickelhaupt, F. M.; Baerends, E. J. Kohn-Sham Density Functional Theory: Predicting and Understanding Chemistry. In *Reviews in Computational Chemistry*; Lipkowitz, K. B., Boyd, D. B., Eds.; Wiley-VCH: New York, 2000; Vol. 15, pp 1–86.

(46) Krapp, A.; Bickelhaupt, F. M.; Frenking, G. Orbital Overlap and Chemical Bonding. *Chemistry* **2006**, *12* (36), 9196–9216. https://doi.org/10.1002/chem.200600564.

(47) Murray, J. S.; Brinck, T.; Edward Grice, M.; Politzer, P. Correlations between Molecular Electrostatic Potentials and Some Experimentally-Based Indices of Reactivity. *Journal of Molecular Structure: THEOCHEM* **1992**, *256*, 29–45. https://doi.org/10.1016/0166-1280(92)87156-T.

(48) Bickelhaupt, F. M.; Sola, M.; Schleyer, P. V. Theoretical Investigation of the Relative Stabilities of XSSX and X2SS Isomers (X=F, Cl, H, and CH3). *J Comput Chem* **1995**, *16* (4), 465–477. https://doi.org/10.1002/jcc.540160410.

(49) El-Hamdi, M.; Poater, J.; Bickelhaupt, F. M.; Sola, M. X2Y2 Isomers: Tuning Structure and Relative Stability through Electronegativity Differences (X = H, Li, Na, F, Cl, Br, I; Y = O, S, Se, Te). *Inorg Chem* **2013**, *52* (5), 2458–2465. https://doi.org/10.1021/ic3023503.